Pol. J. Environ. Stud. Vol. 34, No. 4 (2025), 4143-4153
DOI: *10.15244/pjoes/190012* ONLINE PUBLICATION DATE: 2024-12-16

Original Research

Study on the Stability of Loess Landslides Based on Vegetation Characteristics and the Geo-Studio Model

Lirong He[1, 2, 3], Lei Shi[4, 5], Guobin Liu[1, 2, 3]*

[1]Institute of Soil and Water Conservation, Chinese Academy of Sciences and Ministry of Water Resources, Yangling, Shaanxi, China
[2]Research Center of Soil and Water Conservation and Ecological Environment, Chinese Academy of Sciences and Ministry of Education, Yangling, Shaanxi, China
[3]University of Chinese Academy of Sciences, Beijing, China
[4]Shaanxi Provincial Land Engineering Construction Group Co., Ltd, Xi'an, Shaanxi, China
[5]Technology Innovation Center for Land Engineering and Human Settlements, Shaanxi Land Engineering Construction Group Co., Ltd, School of Human Settlements and Civil Engineering, Xi'an Jiaotong University, Xi'an, Shaanxi, China

Received: 24 March 2024
Accepted: 12 June 2024

Abstract

As the central accumulation area of the Loess Plateau in Shaanxi Province, China, Loess landslides occur frequently, which seriously affect the safety of people's lives and properties. The prediction and early warning of landslides are the hot spots of geological disaster research, and the prediction of the stability of Loess landslides can provide a reference basis for the prevention and management of landslides. This study takes a typical Loess landslide site in Ganquan County, Yan'an City, as the research object. By collecting soil samples from the landslide body for indoor simulation tests and analyzing and testing the changes in the basic physical and mechanical properties of the soil under different plant root densities and different precipitation conditions, the stability of shallow Loess landslides on the Loess Plateau was simulated using Geo-Studio software. The analysis shows that the stability coefficient of the natural root density of Zhangzi slope soil is 0.889, which belongs to the unstable state, and under the condition of 1.5 times root density, its stability coefficient increases to 1.246, which belongs to the stable state, while at 2 times root density, its stability coefficient decreases to 0.973, which belongs to unstable state, and the stability of its root-soil complex is 1.5 times root density > 2.0 times root density > natural root density. Under different soil water content conditions, the stability of the slope shows a trend of decreasing with increasing water content. Under the condition of 10% soil water content, the stability coefficient of the landslide slope is 1.123, which is the basic

*e-mail: sl19890419@foxmail.com;
Tel.: +86 187 1057 7336;
Fax: +86-029-8701-2875

stability state; under the condition of 20% soil water content, the stability coefficient drops to 0.886, which is the unstable state; under the condition of 30% soil water content, the stability coefficient is 0.724, which indicates that precipitation has a great influence on the stability of Loess landslides.

Keywords: loess landslide, slope stability, plant root density, precipitation, geo-studio

Introduction

As the central accumulation area of the Loess Plateau in the northern region of Shaanxi Province, China, landslides are a frequent category of geological hazards in the region, which seriously affects the safety of people's lives and properties as well as the high development of the ecological environment [1, 2]. Due to the relatively low cost of landslide prediction and early warning, it has been a hot topic in the field of landslide geological disaster research in recent years [3–5]. The establishment of a prediction and early warning mechanism for Loess landslides has been included as a key objective in the geological disaster prevention and control plan of Shaanxi Province [6, 7]. Therefore, in view of the actual natural conditions of the Loess Plateau in northern Shaanxi, the establishment of a corresponding Loess landslide prediction and early warning mechanism under the new geological conditions brought about by the ecological management of the Yellow River Basin is an urgent task in the current disaster prevention and control work. This not only helps to deepen the knowledge of the ecological environment in the Loess Plateau region of northern Shaanxi, but also provides a reference basis for landslide geohazard management and promotes the process of ecological civilization construction in China [8-10].

The landslide stability prediction mechanism, as an effective disaster prevention and mitigation measure, is of great significance to the Loess region. Existing prediction and early warning methods make it difficult to achieve the expected results in practical application due to ignoring the spatial differences in the conditions of vegetation cover and soil mechanical properties in different areas [11–13]. This study selects the more typical Loess landslide potential sites in the Loess Plateau and, through field research, takes soil samples to obtain the soil mechanics and hydrological parameters of different vegetation affecting the stability of slopes, combined with the nature of the soil under different vegetation conditions, to summarize the characteristics of Loess slope stability and the response to the vegetation. In this paper, based on the vegetation cover, soil hydromechanical properties, and geomechanical characteristics of the study area, a GeoStudio-based Loess landslide prediction model is established, which makes the system more accurate in predicting the stability of Loess landslides and easier to extend to different scenarios. The results of the study can be applied to Loess landslide disaster prevention and mitigation projects in the Loess Plateau to promote the high-quality development of the Yellow River Basin.

Study Area, Materials, and Methods

Study Area

Ganquan County is located in the central area of Yan'an City, Shaanxi Province (108°45′34 "E – 109°33′46″E, 36°6′57″N – 109°33′46″N), where Loess landslides are frequent. Ganquan County belongs to the typical northern Shaanxi Loess Plateau hilly and gully landscape, with an altitude between 950-1625 m, a semi-humid inland monsoon climate, and an annual rainfall of 126.3 mm. The county area is 2284.7 km^2, and the forest and grass coverage rate reaches 78.4% [14].

The landslide site of Jangzigou is located in Shimen Town, Ganquan County (109°21′53″E, 36°17′55N), and is a Loess landslide that has occurred, with the highest part of the landslide in the shape of a circle chair, the profile form is convex, the overall slope is about 30°, the east-west length is about 95 m, and the north-south length is about 170 m. The relative height difference of the landslide is about 87 m, and the average thickness of the landslide Loess is about 10 m (Fig. 1). The stratigraphic structure is divided into Upper Pleistocene Loess of the Quaternary at the back edge of the landslide, and the main body of the landslide is Upper Pleistocene stacked Loess of the Quaternary with a thick bed of massive feldspathic sandstone, which is a typical Loess-bedrock type landslide [15, 16].

Soil Sample Collection and Remodeling Sample Preparation

In May 2022, field research was carried out in the study area, counting the plant species, number, density, and root distribution in the area, selecting typical Loess landslide potential sites in the area to take Loess soil samples, selecting three main plant types from each slope, and setting up bare ground with similar ground conditions to the sampling site as a control. A 50 cm × 50 cm square soil profile was excavated 50 cm downslope from the base of the tree to collect samples of normal root growth and development and avoid the influence of mechanical force on the root system as much as possible in the collection process. Soil samples were collected using the profile method. In the vertical profile of each shrub sampling point, soil samples were taken in layers every 10 cm; the sampling depth was 50 cm; the mixed sampling method was used in the same soil depth; and the collected samples were sealed and preserved [17, 18].

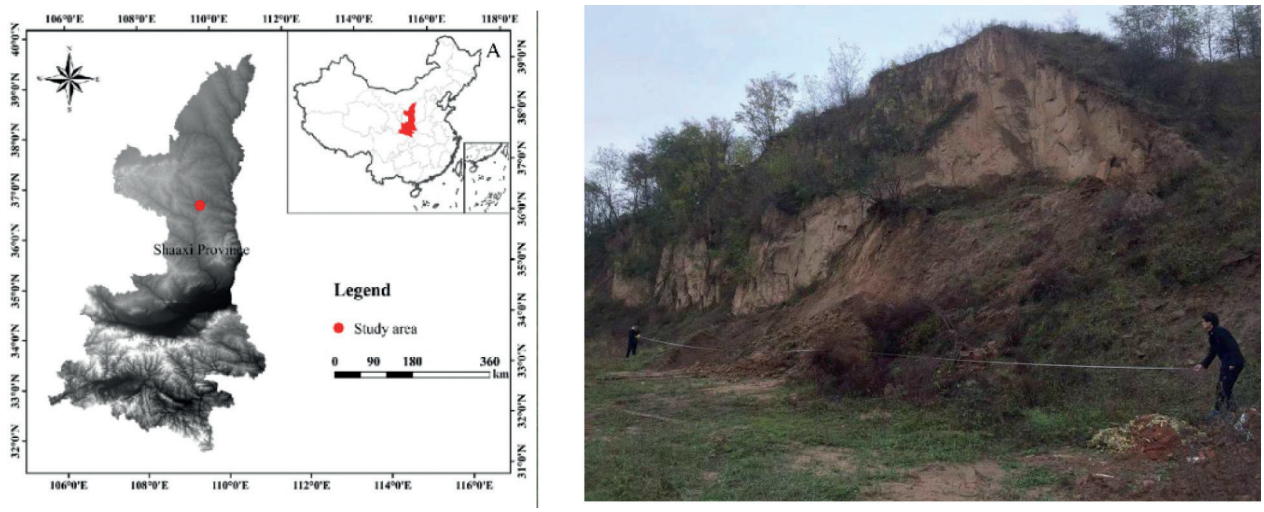

Fig. 1. Landslide point distribution map in Ganquan County.

The collected soil samples were dried and ground, and then sieved through 1 mm. The sieved soil samples were spread in non-absorbent aluminum discs and sprayed with the expected amount of water addition. The amount of water addition was calculated using the formula:

$$m_w = \frac{m}{1 + 0.01\ w_0} \times 0.01(w' - w_0) \qquad \text{Eq. 1)}$$

Where m_w is the amount of water to be added to the soil sample (g), m is the mass of the soil sample at the air-dry moisture content (g), w_0 is the air-dry moisture content (%), and w' is the required moisture content for the design (%) [19].

Data Processing and Analysis

In this study, numerical simulations are carried out based on the vegetation characteristics of landslide hazard points [20–23] and the relevant engineering and geological conditions in the area. According to different rainfall conditions and slope stability, the rainfall threshold for severe landslide instability under various scenarios is analyzed, and this rainfall threshold is used as the forecast and warning threshold. Discuss the change in slope stability and the threshold value of landslide occurrence under different rainfall conditions. In this study, the numerical simulation of slope stability is based on the limit equilibrium method to analyze the occurrence of potential landslides, and the slope stability under different conditions is simulated by inputting relevant soil mechanics information and hydrological parameter information in GeoStudio software [24–26].

GeoStudio is a software widely used in scientific research and engineering construction, and its multi-module integration feature allows coupled analysis of slope seepage conditions and stability [27]. A two-dimensional slope model is established by inputting soil mechanical properties measured in the field into the software and assigning the corresponding hydromechanical parameters. After that, a certain amount of rainfall is set as a landslide inducing condition for the landslide and brought into SEEP/W for seepage simulation to obtain the hydrological changes of a sloped body over a period of time with a given amount of rainfall [28]. The resulting hydrological information is then input into the SLOPE/W module, and the time of landslide damage and the landslide damage surface can be simulated according to the Spencer limit equilibrium method [29]. By comparing the simulation results of typical Loess landslides under different scenarios and setting the rainfall threshold for landslide occurrence according to the critical rainfall intensity and rainfall duration at the time of landslide occurrence, the method of landslide prediction and warning is proposed by combining this threshold with meteorological monitoring means [30–32]. A certain amount of rainfall is set as the landslide inducing condition, and seepage simulation is carried out so as to obtain the hydrological changes of the slope under the rainfall conditions in a certain period of time, and then the obtained hydrological information is input into the SLOPE / W module. By comparing the simulation results of typical Loess landslides under different scenarios, the characteristics of the Loess landslide destabilization process are analyzed. Finally, the rainfall threshold for landslide occurrence is determined based on the critical rainfall intensity at the time of landslide occurrence.

Results and Analysis

Vegetation Community Composition and Root Distribution

Species Composition of the Plant Community

A field survey of the flora of the study area yielded 41 common plant species, most of which belong to the warm

temperate zone in their zonal nature, with the most species of *Rhamnaceae* and *Asclepiadaceae*, each with a total of 9 species, accounting for 40% of the total [33, 34], indicating that the vegetation of the study area is dominated by plants of certain families and the community is relatively simple. The community in the study area is divided into three basic levels: tree layer, shrub layer, and herb layer. Among them, the shrub layer is the most developed, with *Ziziphus jujube*, *Periploca sepium, Caragana sinica (Buc'hoz) Rehder, Sophora davidii (Franch.) Skeels, Thermopsis lanceolata R.Br., Tamarix ramosissima Ledeb., Rosa xanthina Lindl*., and others.

Based on the number of plant species in the sample plots obtained from the survey, the community plant diversity calculation method was used to derive the community evenness index (J_{sw}), diversity index (H′), and ecological dominance index (C) for each sample plot [35]. The measurement method applied in this paper was to calculate the diversity indices of herbs, shrubs, and trees in the plant community separately and summed to derive the community stratified diversity [36]. The overall diversity index of the plant community was calculated using the direct participation of herbaceous, shrub, and tree species in the diversity calculation (Table 1).

Vertical Distribution Characteristics of Vegetation Root Systems

During the vegetation restoration succession in the Loess area, the above-ground part of vegetation and the underground root system continuously restore organic matter to the soil, which promotes the improvement and enhancement of soil physicochemical properties [37]. The improvement of the soil growth environment in turn has an impact on the growth and distribution characteristics of vegetation, which facilitates the invasion of plant species and promotes the development of vegetation succession. As can be seen in Fig. 2, most of the vegetation roots in the study area are concentrated in the 0–40 cm soil layer at the surface, and this root distribution characteristic makes the surface soil gradually dense, changing the loose condition of the soil at the early stage of vegetation restoration [38]. In addition, without the interference of external factors, a layer of deadfall will gradually form under the cover of perennial vegetation, and the joint action of vegetation roots and deadfall makes the surface The combined effect of vegetation roots and litter makes the surface soil free from erosion [39]. However, this dense soil structure also reduces the infiltration capacity of the soil, which is

Table 1. Diversity index of plant communities in landslide areas.

Community Type	J_{sw}	H′	C
I (*Ziziphus jujube* + *Periploca sepium*)	3.1933	3.4745	4.0192
II (*Ziziphus jujubei* + *Ophiopogon bodinier*)	4.0510	3.2176	4.2316
III (*Periploca sepium* + *Caragana sinica (Buc'hoz) Rehder*)	3.9192	3.7332	3.9842
IV (*Periploca sepium*)	3.8124	3.6352	4.1327

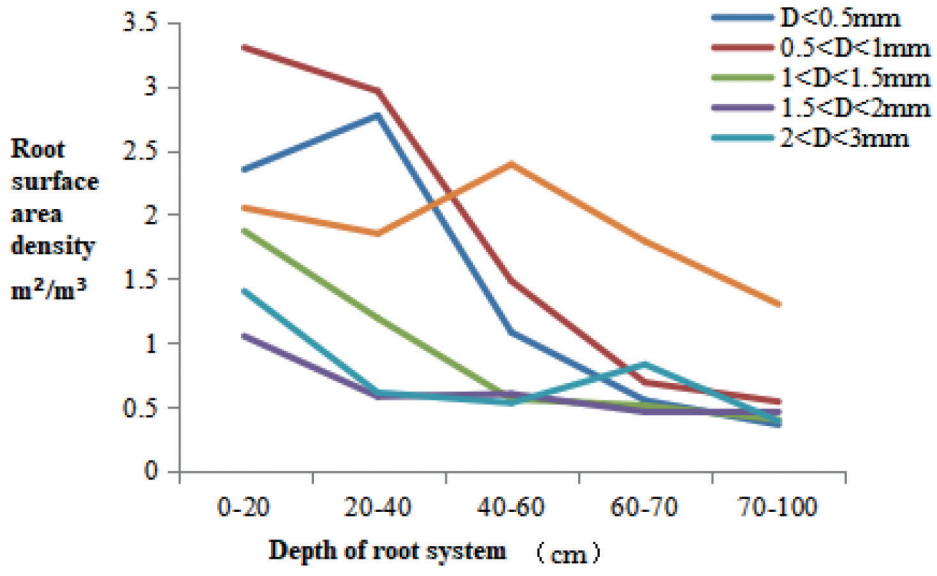

Fig. 2. Root distribution characteristics of vegetation in the study area.

Table 2. The composition of different vegetation communities on the plot.

Community type	Natural moisture content %	Saturated moisture content %	Saturated moisture content g/cm^3	Saturation density g/cm^3	Porosity %
I	14.22	32.95	1.44	1.85	52.6
II	16.82	32.56	1.43	1.82	53.2
III	14.84	26.17	1.49	1.83	50.1
IV	13.65	23.08	1.83	2.08	39.7

Table 3. Vertical infiltration coefficients of soils in different types of vegetation communities.

Vegetation Communities	I	II	III	IV
Vertical permeability coefficient K_{fs} (mm/min)	0.74	0.52	0.98	1.45

not conducive to the utilization and storage of rainwater resources in arid and semi-arid areas [40].

Physical Properties of Soils in Different Types of Vegetation Communities

Based on the soil samples collected from the study area for testing, the results of soil water content and density were obtained (Table 2). The permeability coefficient of the soil in the study area was obtained between 0.52 and 1.45 mm/min, and the size of the vertical permeability coefficient of the soil was: II < I < III < IV (Table 3). The permeability of III and IV is better, which facilitates the infiltration of rainwater, and in addition to this, the emergence of a waterfall hole in III also facilitates the rapid infiltration of rainwater into the soil, which increases the weight of the slope on the one hand and reduces the shear strength of the soil on the other [41].

Landslide Stability Evaluation

Landslide Profile and Computational Profile Construction

In this study, the stability of the landslide at the Zhangzi landslide site in Ganquan County, Yan'an City, was evaluated by using the Spencer method applicable to any slip surface shape, establishing a system of equations satisfying all force and moment balances, iteratively solving for the safety coefficients, and then evaluating the stability of the slope under different conditions [42].

According to the field survey and related geological data, the landslide body is Quaternary Upper Pleistocene Loess with an average thickness of about 10m; the slip zone is a contact zone between Lower Cretaceous sandstone and Loess; and the slip bed is Cretaceous sandstone. Accordingly, the evaluation model of the landslide in Zhangzi is constructed, and the landslide profile is simplified into Loess accumulation, Loess, and bedrock, and the front and profile of the landslide are shown in Fig. 3.

Landslide Profile and Computational Profile Construction

The seismic intensity of the study area is VI degrees, so the influence of earthquakes on landslide stability is not considered [43]. Landslide stability mainly considers the influence of vegetation roots and rainfall, so two cases of different root densities and different soil water contents are taken for simulation analysis. The different root densities simulate the natural surface water content, and the soil water content where the root system of jujube is located is 9.5% after field sampling and analysis, and the natural root density of the jujube is set at 1.5 times the natural root density and 2.0 times the natural root density, where the natural root density of the jujube is 0.85 g/100 g soil [44]. The selected parameters are detailed in Table 4. This outlines root density conditions with soil water content at 10%, 20%, and 30% [45]. The selected parameters are detailed in Table 5.

Calculation Results and Analysis

According to the Code for Landslide Prevention and Control Engineering Survey (DZ/T0218-2006), the stability states of landslides and the corresponding safety coefficients are shown in Table 3 below, and the stability of landslides is evaluated by the stability states corresponding to the safety coefficient values simulated by the model.

The stability coefficients of the slope are calculated by the parameters of different root densities, and the stability of the slope under different root densities is shown in Fig. 4. The calculation results show that under the conditions of different root densities, the stability coefficient of the natural root density of the slope of Zhangzi ditch is 0.889, which is an unstable state, and under the conditions of 1.5 times root density, the stability coefficient of the slope increases to 1.246, which is a stable state, while when the root density increases to 2 times, the stability coefficient of the slope decreases to 0.973, which is an unstable state.

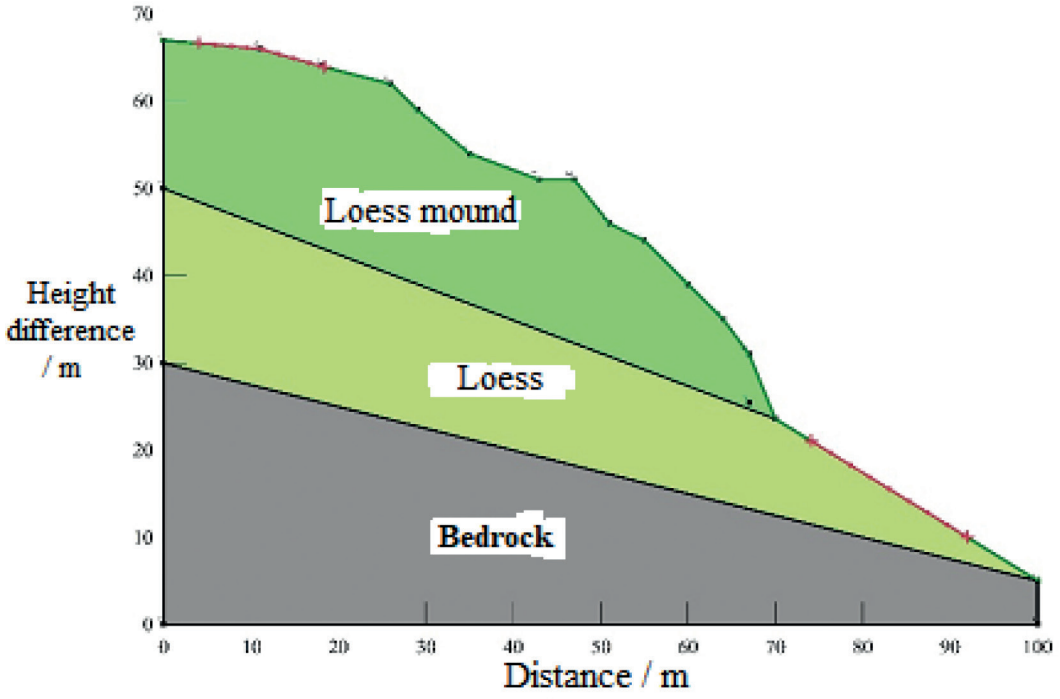

Fig. 3. Topographic profile of the Zhangzi landslidel.

Table 4. Vertical infiltration coefficients of soils in different types of vegetation communities.

Work conditions	Rockiness	Severe (KN/m^3)	Cohesion (kpa)	Angle of internal friction (°)
Different root density	Natural root density	14.0	18.22	18.78
	1.5 times root density	14.0	16.03	35.75
	2.0 times root density	14.0	13.08	25.64
Different soil moisture content	10%	13.9	12.18	32.62
	20%	14.1	7.83	24.23
	30%	14.5	3.57	18.26

Table 5. Landslide stability state grading table.

Stability factor	Unstable	Less stable	Basic stability	Stable
Stable state	Fs < 1.00	1 ≤ Fs < 1.05	1.05 ≤ Fs < 1.15	Fs ≥ 1.15

Under the condition of 1.5 times root density, its slope stability coefficient increases to 1.246, which is stable, and under the condition of 2 times root density, its slope stability coefficient decreases to 0.973, which is unstable. Therefore, for the sour date root system, its root-soil complex shear strength is 1.5 times root density > 2.0 times root density > natural root density.

Fig. 5 shows the simulation results of the landslide in Zhangzi, Ganquan County, under different soil water content conditions. It can be seen from the figure that the stability of the slope under different soil moisture content conditions shows a trend of decreasing with the increase of water content. Under the condition of 10% soil moisture content, the stability coefficient of the landslide slope is 1.123, which belongs to the basic stability state; under the condition of 20% soil moisture content, the stability coefficient plummets to 0.886, which belongs to the unstable state; under the condition of 30% soil moisture content, the stability coefficient is 0.724. This indicates that precipitation has a great influence on the stability of the landslide in Zhangzi. Therefore, for the landslide in Zhangzi, Ganquan County, Yan'an City, rainfall is one of the main factors in the occurrence of this landslide.

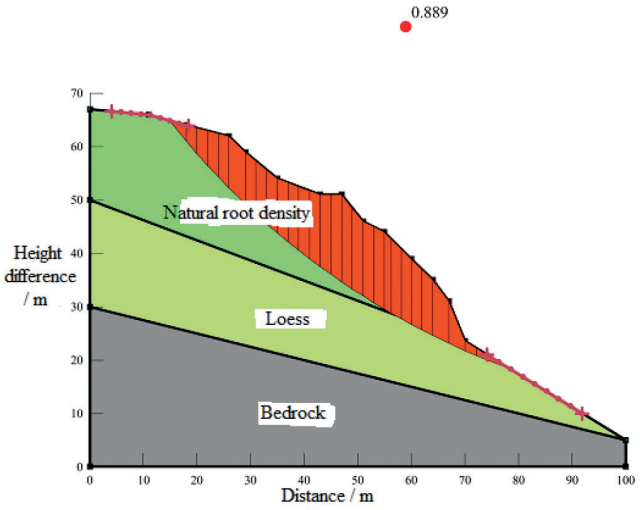

(a): Natural root density.

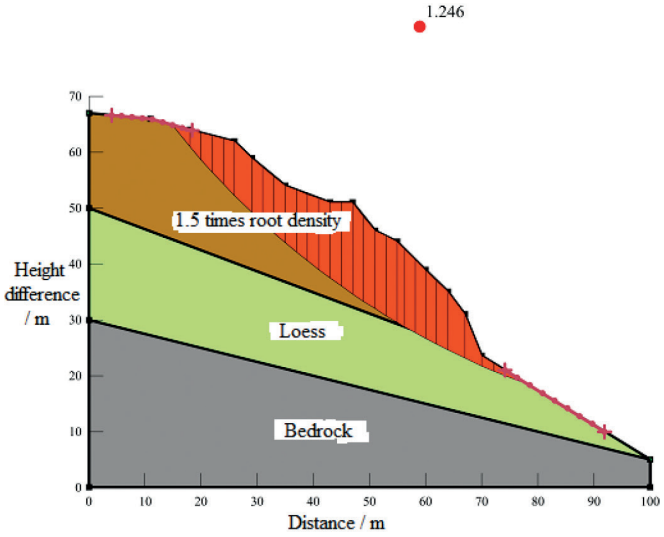

(b): 1.5 times root density.

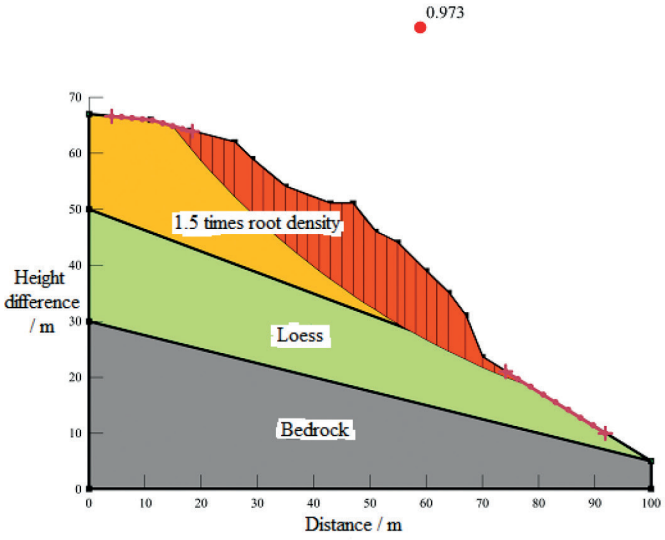

(c): 2 times root density.

Fig. 4. Simulation results of the landslide in Zhangzi, Ganquan County under different root density.

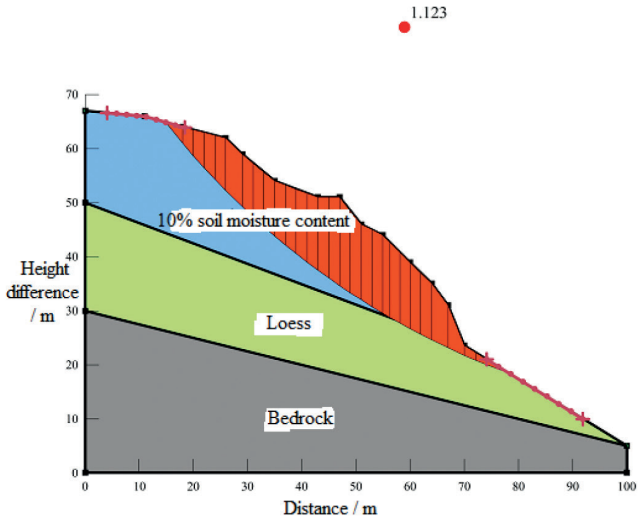

(a): 10% soil moisture content.

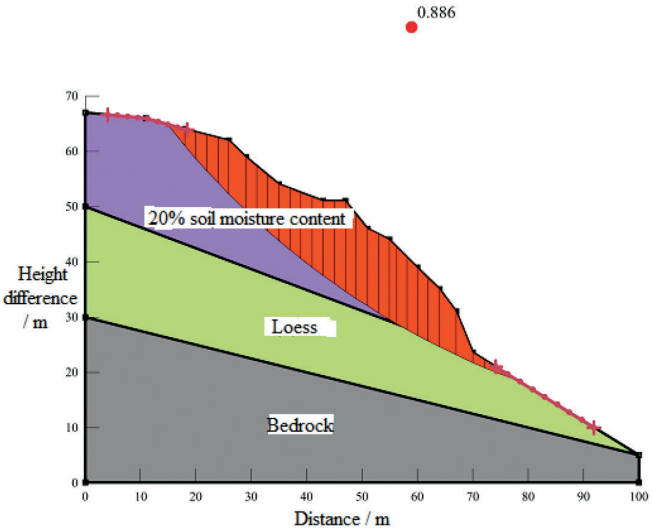

(b): 20% soil moisture content.

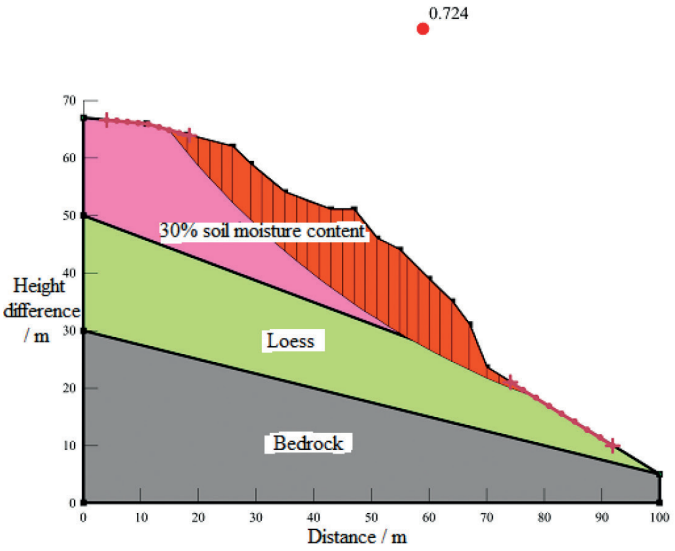

(c): 30% soil moisture content.

Fig. 5. Simulation results of landslide in Zhangzi, Ganquan County under different soil water content conditions.

Discussion

In this paper, some disaster sites in Ganquan County were selected as research cases, and soil samples of landslides in the field were collected and analyzed in indoor experiments to obtain the physical and mechanical properties of the soil under natural and artificial interventions, and Geo-Studio software was used to simulate the stability conditions of landslides under different rainfall conditions.

Landslides are mainly distributed within drylands, medium-coverage grasslands, and low-coverage grasslands, indicating that surface vegetation cover can affect landslide stability, and the number of landslides occurring in places with poorer vegetation cover increases [46]. The basic mechanical properties of landslide body soils indicate that the pore ratio and porosity decrease with increasing dry density, the cohesion of natural soils is significantly higher than that of saturated soils, and the internal friction angle of natural soils is slightly lower than that of saturated soils. Overall, the shear strength of the natural soil samples was higher than that of the saturated soil samples, influenced by the moisture content.

In the three root density gradients set in this study, the highest shear strength of the root-soil complex was found at 1.5 times the natural root density for sour date, and the root-soil complex shear strength was influenced by the root density and was positively correlated with a certain range. The value added of root-soil complex cohesion in this study varied between 2.98% and 127.15%. The water content corresponding to the optimal root density for the shear strength of different plants is different, and when the water content or root density is beyond the optimal range, the root effect on soil shear strength enhancement will be reduced or even disappear and even play a counter effect on slope stability.

Conclusions

In this study, the disaster-prone area of Zhangzi slope in Ganquan County was used as the research object. Geo-Studio software was used to simulate the stability of shallow Loess landslides and monolithic landslides on the Loess Plateau, respectively. The conclusions drawn in the paper are as follows:

1. Under different root density conditions, the stability coefficient of the natural root density of the slope of Zhangzi ditch is 0.889, which is an unstable state, and under the condition of 1.5 times root density, its slope stability coefficient increases to 1.246, which is a stable state, and when it increases to 2 times root density, its slope stability coefficient decreases to 0.973, which is an unstable state, so for the sour date root system, its root-soil complex Therefore, the shear strength of the root-soil complex is 1.5 times the root density > 2.0 times the root density > natural root density.

2. Under the condition of 10% soil moisture content, the stability coefficient of the landslide slope is 1.123, which is the basic stability state; and under the condition of 20% soil moisture content, the stability coefficient plummets to 0.886, which is the unstable state; under the condition of 30% soil moisture content, the stability coefficient is 0.724, which indicates that precipitation has a great influence on the stability of the landslide in Zhangzi.

Acknowledgements

The study was supported by the projects of "The Natural Science Basic Research Plan in Shaanxi Province of China (2024JC-YBQN-0323)".

Conflict of Interest

The authors declare no conflict of interest.

References

1. PU S.R. Constraints and triggering causes of Loess landslides in Shaanxi. Resource Environment and Engineering, **22**, 133, **2008**.
2. ZHUANG J.Q., PENG J.B., ZHANG L.Y. Prediction and evaluation of the risk of shallow landslides on Loess plateau under different rainfall conditions. Journal of Jilin University: Earth Science Edition, **3**, 867, **2013.**
3. GAO J.L., ZHANG J.G. Characteristics of changes in key soil and water conservation measures in Loess hilly gully areas. Soil and Water Conservation Bulletin, **39** (003), 114, **2019**.
4. ZHANG S., JIA HE., WANG C., WANG X., HE S., JIANG P. Deep-learning-based landslide early warning method for loose deposits slope coupled with ground water and rainfall monitoring. Computers and Geotechnics, **165**, 176, **2024**.
5. LIU L., DENG J., YU T. A Dynamic Management and Integration Framework for Models in Landslide Early Warning System. ISPRS International Journal of Geo-Information, **12**, 5, **2023**.
6. SU X., WEI W.H., GUO W.Q. Analysis of the influence of topographic relief on Loess landslides in Tianshui City based on SRTM DEM. Glacial Permafrost, **39** (3), 616, **2017**.
7. LIU Y., HUANG J., XIAO R., MA S., ZHOU P. Research on a Regional Landslide Early-Warning Model Based on Machine Learning-A Case Study of Fujian Province, China. Forests, **13**, 2182, **2022**.
8. KANG C., CHEN W.W., ZHANG F.Y. Application of deterministic model in predicting slope stability in Loess gully area. Geotechnics, **32** (1), 207, **2011**.
9. CHEN M., CAI Z., ZENG Y., YU Y. Multi-sensor data fusion technology for the early landslide warning system. Journal of Ambient Intelligence and Humanized Computing, **14** (8), 11165, **2022**.
10. GUO Y., XU Z., ZHU S., LUO X., XIAO Y. Using distributed root soil moisture data to enhance the performance of rainfall thresholds for landslide warning. Natural Hazards, **115** (2), 167, **2022**.
11. XU Q., PENG D.L., HE C.Y. Research on the theoretical method of monitoring and early warning of sudden Loess landslides, the case of Hefangtai in Gansu. Journal of Engineering Geology, **28** (1), 11, **2020**.
12. HUANG M., WENG H., HONG C., XU X., TAO Z. Novel Intelligent Approach for the Early Warning

of Rainfall-Type Landslides Based on the BRB Model. International Journal of Geomechanics, **22**, 10, **2022**.
13. FUSTOS T., MANQUE R., VÁSQUEZ A., HERMOSILLA S.M., LETELIER G.V. Rainfall induced landslide early warning system based on corrected mesoscale numerical models: an application for the southern Andes. Natural Hazards and Earth System Sciences, **22 (**6), 2169, **2022**.
14. ZHOU F., XU Q., QI X. Study on the mechanism of irrigation-induced sudden Loess landslides. Journal of Mountain Science, **38** (1), 10, **2020**.
15. ZHENG Y.W., LIU H.F. Influence of rainfall on the stability of Loess landslides--a landslide in Ganquan County as an example. Natural Science (Digest Edition), **000** (002), 00169, **2016**.
16. SHI C. Investigation on Soil Fertility of Newly Increased Cultivated Land after Wasteland Improvement in Loess Hilly Region-a Case Study in Ganquan County, Shaanxi Province. IOP Conference Series: Materials Science and Engineering, **394**, 5, **2019**.
17. FAN L.M., LI Y., NING K.B., TENG H.Q., WANG Q.Y., ZHANG X.Y. Small-scale landslides in Loess gully areas cause catastrophes and their mechanisms. Disaster Science, **30** (3), 14, **2015**.
18. CÉLINE L.N.M.B., OLIVIER C. Does a decade of soil organic fertilization promote copper and zinc phytoavailability? Evidence from a laboratory biotest with field-collected soil samples. The Science of the Total Environment, **906**, 167771, **2023**.
19. CHANG C.Y., BO J.S., LI X.B., QIAO F., YAN D.H. A BP neural network model for predicting slip distance of seismic Loess landslides. Journal of Earthquake Engineering, **42** (6), 6, **2020**.
20. LONG J.H., NI X.L., ZHAO B.Q., ZHANG J.N. Analysis of the landslide mechanism of a large vegetation-filled site in a Loess ravine. Journal of Natural Hazards, **29** (6), 8, **2020**.
21. CHEN Q., CUI D.S., WANG J.G., LIU Q.B. Experimental study of creep in landslide zone soils of Loess slopes under different consolidation conditions. Geotechnics, **41** (5), 8, **2020**.
22. JIE F., FAN Y., CHENG J., WU H. The Spatio-Temporal Evolution Characteristics of the Vegetation NDVI in the Northern Slope of the Tianshan Mountains at Different Spatial Scales. Sustainability, **15**, 8, **2023**.
23. TAKEHIRO O., ATSUSHI H., TOMOYUKI T., AKIHIRO K. Topographical Attribute and Vegetation Change on Increase of Topography of Landslide Disaster. Journal of the Japan Society of Engineering Geology, **49** (4), 204, **2008**.
24. YANG S., CHANG C.Y., LI X.B., HAN X. A rapid evaluation method for seismic stability of Loess slopes based on logistic regression model. Journal of Earthquake Engineering, **42** (2), 5, **2020**.
25. LI W.Y., WANG X.L. Application and comparison of frequency ratio and information quantity models in the evaluation of landslide susceptibility in Loess gully areas. Journal of Natural Hazards, **29** (4), 8, **2020**.
26. AMIN M.N. Computer-Aided Slope Stability Analysis of a Landslide – A Case Study of Jhika Gali Landslide in Pakistan. Sustainability, **14** (20), 12954, **2022**.
27. ZENG C.L., LI R., GUAN X.D., ZHANG S., BAI W.S. Experimental study of rainfall infiltration characteristics of Loess slopes under different rainfall intensities. Journal of Geotechnical Engineering, **1**, 5, **2020**.
28. YANG L., MOU X.L., LI C., ZHENG X., YUE D.X. Evaluation of geological hazard risk in Baota District, Yan'an City. Journal of Mountain and Earth Sciences, **38** (5), 12, **2020**.
29. DAI Z.S., WANG Y.Q., MA C., WANG Y.J., WANG X.H., LI M.Y. Dynamic slope stabilization effect of acacia in Loess hills and gullies. Journal of Soil and Water Conservation, **34** (5), 9, **2020**.
30. HUANG J.K., WANG X.L., J.N., CHEN L.H., ZHANG Z.W. Simulation of soil consolidation effect of herbaceous plants on Loess plateau based on asymptotic homogenization theory. Journal of Agricultural Engineering, **36** (9), 9, **2020**.
31. TAHA T.A., YUKSEL Y. Hydro-Mechanical Behaviour of a Rainfall-Induced Landslide by Instrumental Monitoring: Landslide - Rainfall Threshold of the Western Black Sea Bartin Region of Türkiye. Applied Sciences, **13**, 15, **2023**.
32. DOU H., WANG R., WANG H., JIAN W. Rainfall early warning threshold and its spatial distribution of rainfall-induced landslides in China. Rock Mechanics Bulletin, **2**, 3, **2023**.
33. ZHU W.F., ZHAO C., ZHANG Q., KANG Y. Identification and monitoring of Hefangtai Loess landslide using InSAR. Survey and Mapping Science, **44** (5), 7, **2019**.
34. FENG T., QI Y., ZHANG Y., FAN D., WEI T. Long-term effects of vegetation restoration and forest management on carbon pools and nutrient storages in northeastern Loess Plateau, China. Journal of Environmental Management, **354**, 120296, **2024**.
35. FAN C., TANG F., TAN Q.W., YANG Y.M., WEN T. Slip zone soil ring shear test and its insight into the proslide strength of reservoir landslides. Journal of Geotechnical Engineering, **41** (9), 9, **2019**.
36. SHEN Y.D., QIU N., HU S., LIU Z.J., ZHANG Y., YANG D., CAO M. Hydrogeological structure detection and failure cause analysis of Loess plateau landslides. Quaternary Research, **39** (6), 11, **2019**.
37. ZHANG S., PEI X.J., HUANG R.Q., ZHANG X.C., CHANG Z.L., ZHANG Z.D. Model tests on rainfall infiltration characteristics and deformation damage modes of Loess fill slopes. Chinese Journal of Highways, **32** (9), 11, **2019**.
38. SUN P.P., ZHANG M.S., CHENG X.J., HUANG Y.H., XUE Q., LIU J. Occurrence patterns of geological hazards on the Loess Plateau. Journal of Mountain Science, **37** (5), 10, **2019**.
39. BAI Z.N., PENG L., SHEN Y., LI J.G., ZHENG L.C. Characteristics and mechanism of the Zhangjiawan mega-landslide in Xining. Science, Technology and Engineering, **3**, 927, **2021**.
40. XIE W.L., TENG H.Q., DU L., GAI H.L., CHENG T.E., HUANG B. Application of GIS-based combined with fuzzy information method in hazard hazard zoning--a case study of avalanche slide geological hazards in Daxian area. Disaster Science, **33** (3), 6, **2018**.
41. LI R.W., WANG N.Q. Coupling analysis of geological hazards and influencing factors in Yan'an City. Science, Technology and Engineering, **19** (17), 7, **2019**.
42. LI Y.H., LIU H.N., FAN L.M., HE W.Z., JI Y.W., ZHAO Z.H. Distribution pattern of geological hazards in the fragile ecological environment of Yushenfu, Shaanxi. Chinese Journal of Geological Hazards and Prevention, **3**, 6, **2016**.
43. CAI H.E., ZHANG J.W., QIN G.P., TANG H. Analysis of geological hazard susceptibility in Yan'an Loess hilly gully area. Journal of Earthquake Engineering, **37** (B07), 6, **2015**.
44. QIU H.J., CUI P., CAO M., LIU W., GAO Y., WANG Y. Min. Research on the scale frequency distribution

of geological hazards in Loess hilly areas based on the principle of maximum entropy. Geotechnics, **35** (12), 10, **2014**.
45. HUANG Y.H., WU W.Y., FENG W., LI Z.G. Major types and characteristics of geological hazards induced by the "7.3 rainstorm" in Yan'an, northern Shaanxi. Northwest Geology, **3**, 140, **2014**.
46. YIN C., MENG H., LIAN J.F., ZHAO W.J. Response of geohazards to climate change based on different time scales. Geological Review, **59** (6), 1110, **2013**.